

A Solution to the Inverse Problem in Ocean Acoustics

T.V. Ramana Murty, Y.K. Somayajulu, R. Mahadevan
C.S. Murty and J.S. Sastry

National Institute of Oceanography, Goa-403 004

ABSTRACT

The methodology and software developed to reconstruct a vertical sound speed profile as a part of studies on the marine acoustic modelling, using the ray path lengths and the travel time perturbations in tomographic layers are outlined. For a stratified ocean, considering the range independent nature of the medium, geophysical inverse techniques are employed to reconstruct the sound speed profile. The reconstructed profile for a six layer ocean, with five energetic modes, is in good agreement with that of the assumed profile thereby indicating the usefulness of the model. The effect of noise caused by the excursions of the source and receiver moorings; When expressed in terms of travel-time differences, results in the sound speed changes up to 0.1 per cent.

1. INTRODUCTION

Ocean acoustic tomography is a remote sensing tool for screening the interior structure of the ocean, layer by layer, utilising the propagation characteristics of sound waves in the ocean¹. One of the many important features of the ocean is the presence of the sound channel which acts as a waveguide (Fig.1). This channel, also called SOFAR channel, enables propagation of sound over large distances along wholly refracted paths traversing through many layers of the sea. Acoustic rays passing through diverse layers of the ocean interior, therefore, contain history of these layers through which they transgress. Decoding these signatures as received at the acoustic sensors situated at known distances from the sources of origin of known sound signals leads to an understanding of the interior structure of the oceans. This can be examined by simulation of acoustic models or by conducting field experiments using acoustic transmitters and receivers mounted on mooring systems.

The acoustic modelling consists of a study of forward and inverse problems. In the forward problem perfect boundary conditions are used to step a system forward

in time and space. The results can be summarised in terms of the solution of partial differential equations.

In the present study, the reference sound speed profile as a function of depth, for a uniformly deep and layered ocean, forms the input for integrating the partial differential equations (for a given domain) to estimate the ray parameters (Fig. 1). These parameters include the ray path length, and travel time of acoustic pulse along different rays connecting the source and the receiver. The information on travel time perturbations and data kernel comprising ray path lengths for a reference ocean result from the forward model.

In the inverse problem², the model parameters are inferred, given a set of observations consisting of travel time perturbations and the noise statistics over an interior domain and the boundaries.

2. RAY ACOUSTICS

The sound propagation in the sea has been described by a linear, second order, partial differential equation³ in the scalar form known as the wave equation.

$$\nabla^2 \phi = \frac{1}{C^2} \frac{\partial^2 \phi}{\partial t^2} \quad (1)$$

Received 8 January 1991, re-revised 6 August 1991

* Ocean Engineering Centre, IIT, Madras-600 036

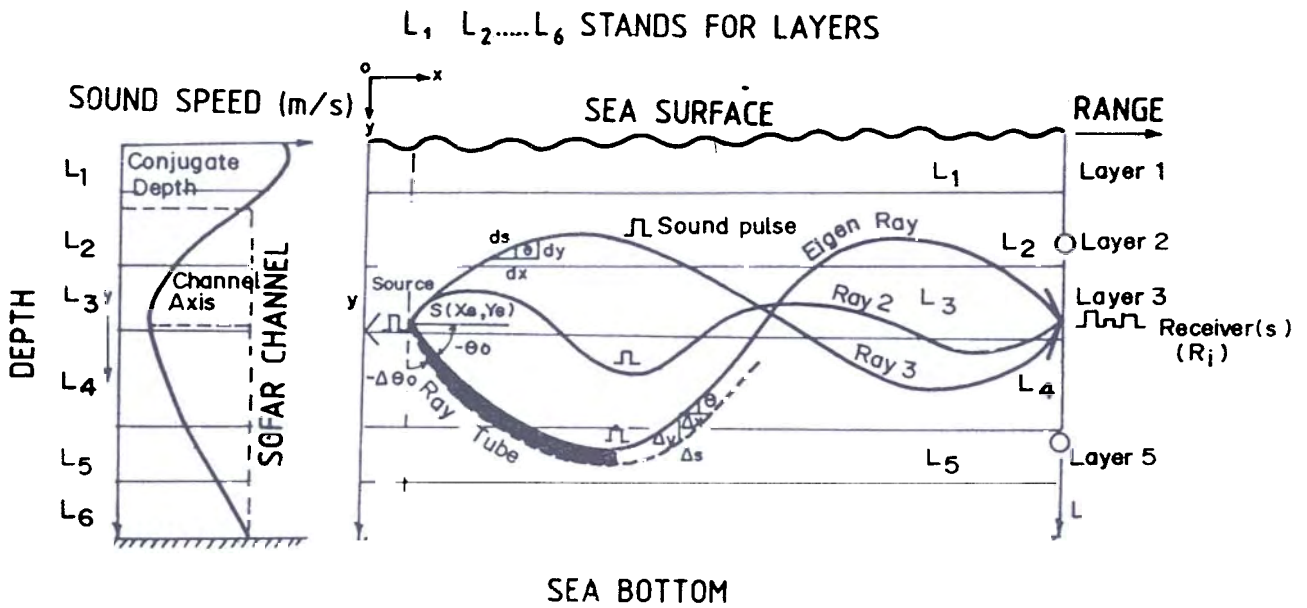


Figure 1. Schematic presentation of acoustic rays from source to receiver.

where ϕ is a potential or a pressure perturbation and C is the speed of sound [$C = C(x, y, z, t)$]—a function of space and time.

Equation (1) can be solved following either the wave theory or ray theory. In the wave theory, functional solutions of linear, second order, partial differential equations for assigned boundary conditions are sought using standard techniques⁴ while the ray theory pertains to solving 'eikonal equation' associated with wave fronts (eikonal is a surface in three-dimensional space). An equivalent way of formulating the ray theory is based on Fermat's principle—path of minimum travel time—for getting the trajectory of the sound pulse or signal. Both eikonal and Fermat's procedures lead to the basic Snell's law of wave refraction.

In the present study, the ray theory has been preferred due to its simplicity and the convenience with which the inverse problem could be tackled. The basic equations governing the ray path, in two-dimensional space are given by³

$$\frac{d}{ds} \left(\frac{n dx}{ds} \right) = \frac{\partial n}{\partial x} \quad \frac{d}{ds} \left(\frac{n dy}{ds} \right) = \frac{\partial n}{\partial y} \quad (2)$$

$$\text{where } dx/ds = \cos \theta \text{ \& } dy/ds = \sin \theta \quad (3)$$

x and y are independent variables representing rectangular spatial coordinates, C is the dependent variable ($C = C(y)$), s represents the arc length along

the ray, n is the index of refraction, and θ is the angle of the ray wrt the horizontal (Fig. 1).

These equations are numerically implemented as explained in the following.

Using Eqn (3) and refractive index $n = C_0/C$, Eqn (2) is expressed as

$$\begin{aligned} \cos \theta \frac{dC}{ds} - C \frac{d}{ds} \cos \theta &= \frac{\partial C}{\partial x} \\ \sin \theta \frac{\partial C}{\partial y} - C \frac{d}{ds} \sin \theta &= \frac{\partial C}{\partial y} \end{aligned} \quad (4)$$

following chain rule

$$\begin{aligned} \frac{d}{ds} \cos \theta &= -\sin \theta \frac{d\theta}{ds} \quad \text{and} \\ \frac{d}{ds} \sin \theta &= \cos \theta \frac{d\theta}{ds} \end{aligned} \quad (5)$$

now,

$$\begin{aligned} \frac{dC}{ds} &= \frac{\partial C}{\partial x} \frac{dx}{ds} + \frac{\partial C}{\partial y} \frac{dy}{ds} \\ &= \cos \theta \frac{\partial C}{\partial x} + \sin \theta \frac{\partial C}{\partial y} \end{aligned} \quad (6)$$

Substitution of Eqns (5) and (6) in Eqn (4) leads to

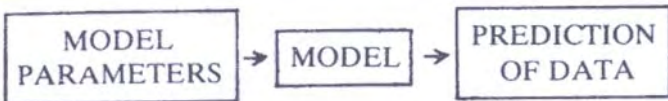
$$\frac{d\theta}{ds} = \frac{1}{C} \left(\sin \theta \frac{\partial C}{\partial x} - \cos \theta \frac{\partial C}{\partial y} \right) \quad (7)$$

Now, the ray travel time is

$$T = \int_{\Gamma_i} [C(s)]^{-1} ds \quad (8)$$

The above equations govern the ray path geometry and sound pulse travel time along the ray paths.

Based on the above acoustic model, forward problem is defined as the process of predicting the results of measurements on the basis of a general model and a set of specific conditions relevant to the problem at hand. In a nutshell, this is expressed as



Each ray traces a unique path as determined by the angle of emergence at the source. A single pulse emitted at the source reaches the receiver as an ensemble of multiple rays, arrival time for which differs by few milliseconds. The (refracted) eigen rays—connecting the source and receiver—computed from the reference sound profile (Fig. 2) are shown in Fig. 3, while the

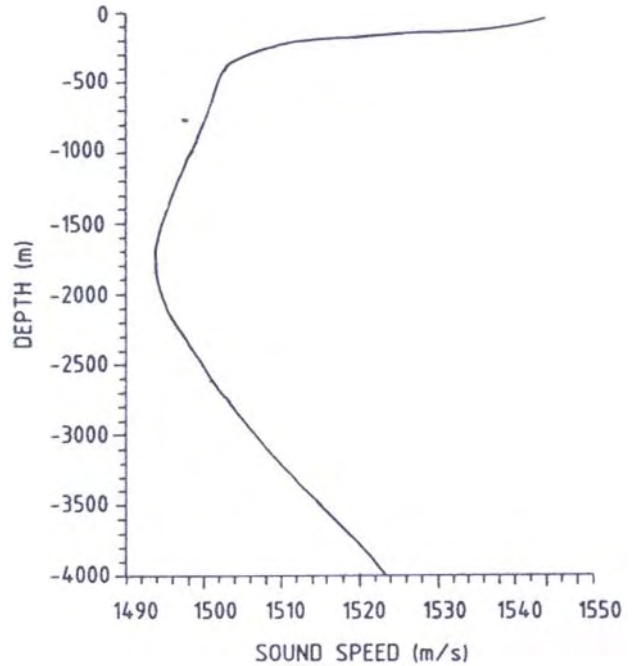


Figure 2. Reference sound speed profile for the Arabian Sea.

various ray parameters computed are presented in Table 1.

Inverse problem helps determine estimates of the model parameters.

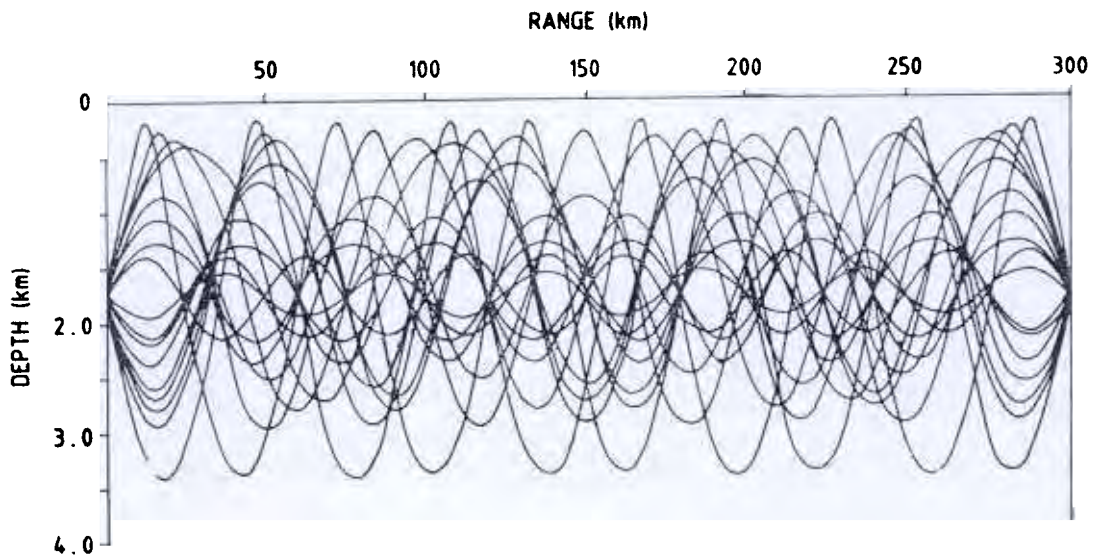
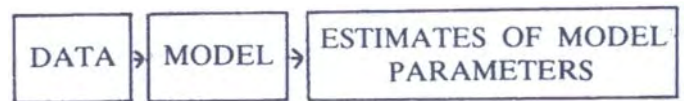


Figure 3. Eigen ray plot.

Table 1. Acoustic ray parameters

Source angle (deg)	Loop length (km)	Fractional length (km)	No. of loops and rays and rays identific 1	Turning depth 1 (m)	Sound speed and turning velocity 1 (m/s)	Turning depth 2 (m)	Sound speed and turning velocity 2 (m/s)	Path length (km)	Travel time (s)	Ray arrival angle (deg)	Ray termination depth (m)
8.7967	60.066	59.738	4 (5,-5)	- 188.10	1511.60	-3281.83	1511.61	302.081	201.0966		-1800.63
7.0020	66.221	35.116	4 (5,-4)	- 282.60	1505.10	-2886.63	1505.13	301.310	200.9317		-1799.98
6.3066	75.114	74.658	3 (4,-4)	- 341.47	1502.99	-2739.24	1502.99	300.969	200.7605		-1800.29
5.7016	75.123	74.631	3 (4,-4)	- 575.46	1501.33	-2617.83	1501.33	300.796	200.7528		-1799.05
4.8826	65.370	38.520	4 (5,-4)	- 830.88	1499.35	-2462.71	1499.34	300.678	200.8604		-1800.09
3.9471	60.144	59.425	4 (5,-5)	-1065.85	1497.45	-2313.63	1497.45	300.525	200.9081		-1799.51
2.9263	60.195	59.220	4 (5,-5)	-1270.03	1495.85	-2156.09	1495.85	300.366	200.9112		-1799.61
2.0008	50.237	48.814	5 (6,-6)	-1479.72	1494.81	-2017.08	1494.81	300.285	200.9428		-1799.27
-0.7949	46.805	19.172	6 (6,-7)	-1847.41	1494.04	-1652.17	1494.04	300.213	200.9484		-1799.76
-1.9559	49.755	1.470	6 (6,-6)	-2010.88	1494.77	-1487.14	1494.77	300.283	200.9451		-1799.72
-3.3022	59.829	0.856	5 (5,-5)	-2216.86	1496.38	-1189.44	1496.38	300.423	200.9149		-1799.22
-3.9300	59.853	0.737	5 (5,-5)	-2311.19	1497.42	-1070.43	1497.42	300.525	200.9126		-1800.51
-5.3864	67.976	28.097	4 (4,-5)	-2557.09	1500.52	- 696.82	1500.53	300.779	200.8366		-1800.86
-5.6972	74.875	0.097	4 (4,-4)	-2616.76	1501.31	- 577.52	1501.32	300.800	200.7594		-1799.64
-6.3147	74.889	0.445	4 (4,-4)	-2740.92	1503.02	- 340.40	1503.01	300.976	200.7675		-1799.26
-6.9011	67.208	31.168	4 (4,-5)	-2865.51	1504.79	- 289.14	1504.78	301.237	200.8791		-1800.22
-8.8685	59.935	0.325	5 (5,-5)	-3303.91	1511.98	- 185.65	1511.91	302.124	201.1069		-1800.73

Source depth (m) = -1750; Receiver depth (m) = -1800; Range (km) = 300

In the present context, the inverse problem is to use the acoustic travel times along resolvable ray paths and any other data (amplitudes could also be used) to obtain an estimate of the model perturbation, i.e., sound speed perturbation, against a reference profile.

The travel time differences (between predicted and observed through field experiment) of sound signals are operated by the generalised inverse operators² for reconstruction of sound speed fluctuations.

3. MATHEMATICAL FORMULATION OF INVERSE PROBLEM

Inverse methods have been treated widely for a variety of problems in geophysical literature⁵⁻⁷ for determining the distribution of some parameters in the earth's interior. The generalised inverses and the regularising techniques are used in these studies to measure quantities on the earth's surface that are functionals of the distribution of physical parameters at depth. Many papers have also appeared on the application of inverse methods to ocean circulation studies⁸⁻¹⁰, using known field of horizontal density gradients to compute geostrophic velocity. The

application of inverse methods in ocean acoustic tomography has been suggested by Munk and Wunsch¹ and later implemented by Cornuelle¹¹, and Cornuelle, *et al*¹².

Considering a single source-receiver system, separated by few hundred kilometers, with eigen rays covering *i* paths and *j* layers located in a stratified ocean, close to the (deep) sound channel axis, the travel time along a ray path *i* is given by

$$T_i = \sum_j R_{ij} / C_j$$

where R_{ij} is the path length of ray *i* in layer *j* and C_j is the sound speed corresponding to layer *j*.

The general model of sound speed field can be written as

$$C(x,y,z,t) = C_o(z) + \delta C(x,y,z) + \Delta C(x,y,z,t)$$

where $C_o(z)$ is the mean reference sound speed, the deterministic refractive term, $\delta C(x,y,z)$ represents the

departure in sound speed due to mesoscale eddies and fronts which can be modelled deterministically and $\Delta C(x,y,z,t)$ indicates the random fluctuations caused by internal wave phenomena, small scale turbulence, etc. The approximate size scales are $C_0 \approx 1500 \text{ m}^{-1}$, δC smaller than C_0 by a factor 10^{-2} and ΔC much smaller by a factor 10^{-4} than C_0 . The last term for modelling the mesoscale phenomena, however, is neglected. For a range independent case such as the one considered here, the problem becomes limited to the estimation of $\delta C(z_j)$ where j indicates the number of layers.

The inversion procedure developed here is based upon the assumption that the perturbation in sound speed is much less compared to the mean sound speed ($\delta C/C_0 \ll 1$). Similarly, the departure of the perturbed path from the reference path is negligibly small ($\delta \Gamma_i/\Gamma_{io} \ll 1$, where Γ_i is the path length of ray i).

Thus for a given i number of identifiable eigen ray paths and j number of layers, one obtains, unknowns in δC_j , viz, number of layers (NL) and linear equations having number of eigen rays (NR), in the matrix form

$$A\delta C = \delta T, \delta C = \delta C_j, \delta T = \{\delta T_i\} \quad (11)$$

where A is data kernel ($-R_{ij}/C^2$) obtained from the initial (forward) model, set in a matrix form, δT_i are deviations of the measured travel times from the reference values, and δC_j are desired model parameter perturbations in the form of a column vector which are to be determined.

The system in Eqn (11) can be separated into (i) over-determined problem (more data than unknowns), (ii) even-determined problems (same number of equations as unknowns), and (iii) under-determined problems (more unknowns than data). The solutions of the equation are of the form

$$\text{Over-determined case: } \delta C = (A^T A)^{-1} A^T \delta T \quad (\text{minimises data error})$$

$$\text{Even-determined case: } \delta C = (A^{-1}) \delta T$$

$$\text{Under-determined case: } \delta C = A^T (A A^T)^{-1} \delta T \quad (\text{minimizes model error})$$

Least square method solves the completely over-determined problem by minimising the squared Euclidean length, i.e., $e^T e$ [where $e = \delta T - A \delta C$], and has a perfect model resolution, i.e., $A^{-1} A = I$. The

even-determined case will have only one solution with no estimation error. Minimum length ($\delta C^T \delta C$ is as small as possible) method solves the completely under-determined problem and has a perfect data resolution, i.e., $AA^{-1} = I$. Generalised inverse $(A^\#)$ that solves the intermediate, mixed-determined problems will have data and model resolution matrices that are intermediate between these two extremes².

So far, the solutions of different types of system of equations and usefulness of the generalised inverse solution have been described. In the following, the construction of the generalised inverse operator using singular value decomposition (SVD) employing the eigen function technique has been considered. The advantages of this technique are: (i) it is objective and does not impose a pre-determined form to the data, (ii) provides an objective means of ranking uncorrelated modes of variability to determine weak signals or noise from the data, and (iii) provides the modes of variability which are not correlated with one another.

SVD is a factorisation of the operator matrix (A) into a set of orthonormal eigen vectors and associated eigen values. The observations are decomposed into linear combination of orthogonal eigen vectors, which in turn determine a linear combination of model parameters. Comprehensive reviews could be seen from the works of Wiggins⁶, Lanczos¹³, Jackson¹⁴, Wiggins *et al*¹⁵, Wunsch¹⁶ and Tarantola¹⁷.

4. GENERALISED INVERSE SOLUTION

Equation (11) is solved by SVD of the matrix A consisting path lengths of eigen rays i in each of the layers j expressed as a product of three matrices^{2,13,18}

$$A = U I V^T \quad (12)$$

$(NR \times NL) \quad (NR \times R) \quad (R \times R) \quad (R \times NL)$

where NL is the number of (tomographic) layers, and NR is the number of resolvable rays.

The columns of the U and V matrices are orthonormal, i.e., $U^T U = I$ and $V^T V = I$. U and V are the respective coupled eigen vector matrices for the eigen value problems defined as

$$(A A^T) u = I^2 u \quad (3)$$

$$(A^T A)v = \dots v \quad (14)$$

In Eqn (12) Γ is a diagonal matrix of non-zero singular values (I^2) of A , and R ($R \leq \min(NL, NR)$) is the rank of the matrix A . Obviously the rank of all the three component matrices will be R and hence all diagonal elements of Γ are squares of the singular, non-zero values. Here, the computational details of the SVD of a rectangular matrix alone are outlined since only standard numerical routines^{4,19} exist to compute the eigen values and corresponding eigen vectors of square matrices.

In general, the number of layers in the ocean is usually less than the number of eigen rays. This leads to a situation of over-determinacy which arises when one attempts to predict the data. It would be also much easier to solve the first eigen value problem (Eqn 13) than the second (Eqn 14).

Equation (13) yields U and Γ , while V is calculated using the equation

$$V^T = \Gamma^{-1} U^T A \quad (15)$$

Having got U , Γ and V , the model parameter δC can be determined. Premultiplying Eqns (13)-(15) by U^T , the following is derived

$$\begin{aligned} U^T A \delta C &= U^T \delta T \\ \Rightarrow U^T U \Gamma V^T \delta C &= U^T \delta T \\ \Rightarrow V^T \delta C &= U^T \delta T \\ \Rightarrow V^T \delta C &= \Gamma^{-1} U^T \delta T \end{aligned} \quad (16)$$

Premultiplying the Eqn (16) with V we get

$$\delta C_p = V V^T \delta C = V \Gamma^{-1} U^T \delta T \quad (17)$$

If $V V^T$ equals I (if the rank of the matrix $A = NR$), the solution of Eqn (11) is

$$\delta C_p = \delta C = (V \Gamma^{-1} U^T) \delta T = (A_p^{-1}) \delta T \quad (18)$$

If $V V^T = I$ (a case in the presence of noise in model space)

$$\delta C_p = \delta C = (V \Gamma^{-1} U^T) \delta T = (A_p^{-1}) \delta T \quad (19)$$

For better estimates the resolution in the model space $V V^T$ of Eqn (19) is improved. This is done by judiciously selecting the p eigen vectors or ranking the singular values of the data kernel in a descending order. The noise in the data kernel (matrix A) prevailing in the form of small eigen values increases the rank of the matrix apart from amplifying the solution. This, however, does not provide any additional or useful information on the sound speed perturbation. So, it can be trusted that the solution to the present problem is obtained through considerations of optimisation.

So far the solution for the generalised inverse pertains to the case of noise-free environment. In the following, solutions where acoustic noise cannot be overlooked particularly while making field observations, have been considered.

5. SOLUTION IN THE PRESENCE OF NOISE

In the acoustic field experiments, uncertainties prevail in the range estimations between the source(s) and receiver(s) over the observation time. These are due to the presence of currents at various level surfaces, along the vertical, eddies of various sizes, internal waves, etc that cause undesirable vertical and horizontal excursions of the moorings. Such movements (10 to 20 m over 4000 m in the vertical and 25 to 50 m over 500 km along the horizontal) though small, apparently contribute to changes in the ray arrival times, and in turn, in the model parameter (δC). With the help of accurate position keeping systems such as the inclinometers and bottom mounted acoustic transponders, these errors could be minimised. The results could be improved further by incorporating a correction factor for travel-time data in Eqns (18) and (19).

The true travel-time data could be considered as the sum of perturbation and noise in the travel time. That is

$$\delta T_{\text{true}} = \delta T_{\text{obs}} + \epsilon \quad (20)$$

Operating generalised inverse operator on either sides of Eqn (20) the following solution is obtained.

$$\begin{aligned} V_p \Gamma_p^{-1} U_p^T (\delta T_{\text{true}}) &= V_p \Gamma_p^{-1} U_p^T (\delta T_{\text{obs}}) \\ V_p \Gamma_p^{-1} U_p^T (\epsilon) & \end{aligned} \quad (21)$$

The sequence of operations of the above procedure in the form of a flow chart is given in Fig. 4.

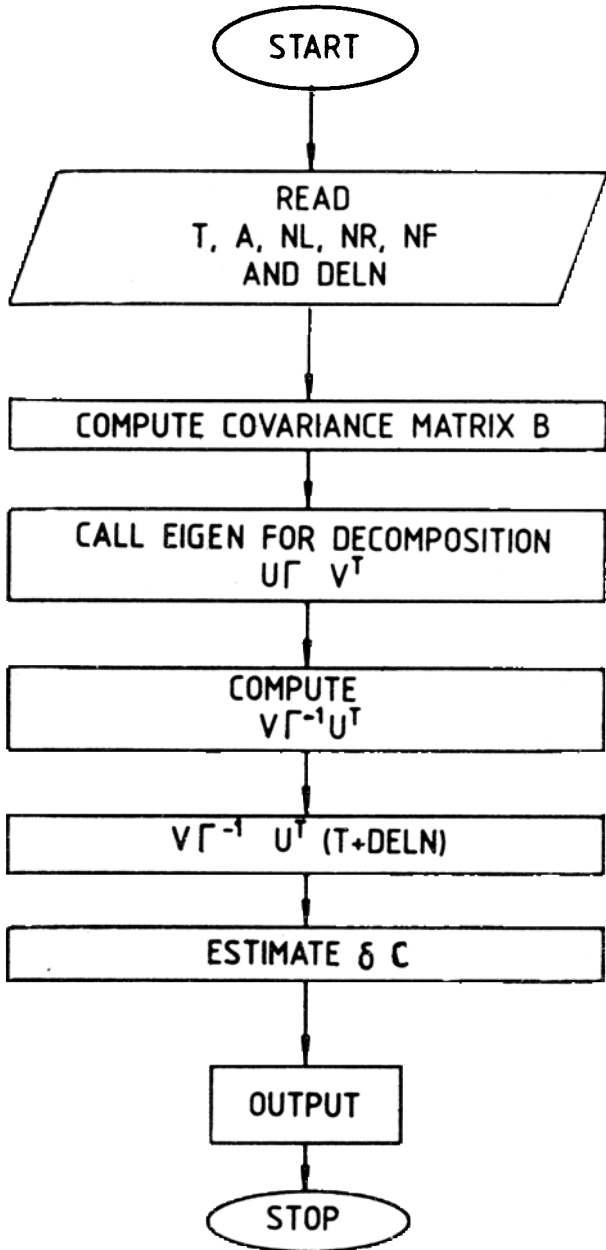


Figure 4. Flow chart of sequence of operations for the procedure in Eqn (21).

Closeness ratio: The ratio between the sum of the factor model and that of the data matrix is considered as the measure of closeness of the model data.

$$\text{Measure of closeness} = \frac{\sum_{i=1}^k l_i^2}{\sum_{i=1}^p l_i^2} \quad (22)$$

where k is the number of factors and p is the rank of the data matrix A (kernel). The eigen functions associated with the largest eigen value represents the data best in the least square sense, while the second

function (in rank) describes the residual mean square data. The closeness ratio is expressed in percentage in order to enable one to judge the contribution of different modes, arranged in descending order, for better reproduction of the model profile.

6. VALIDATION OF THE MODEL

From the technological point of view, preliminary tests need to be carried out before the conduct of a practical tomographic study. These tests include demonstration of some essential properties of ocean for long range propagation. Of these tests, resolving the rays (eigen rays) and means to observe and identify them to sufficient accuracy is amongst the most desired. These rays must also be checked for their stability. Various measurement errors are to be estimated.

For identification of the rays, one must compare the observed pattern with a prediction based on available sound speed profile—archived or exclusively collected. This would enable realisation of the fact that some peaks would be attenuated and some unresolvable. For ray prediction and identification, the mean profile is used.

In the present study, environmental hydrographic data from the Arabian Sea, available in the form of seasonal mean values of temperature and salinity at standard oceanographic depths has been utilised to test the software in respect of the acoustic model described hitherto. Using the internationally accepted formula of Chen and Millero²⁰ for the determination of sound speed based on this data, vertical profiles depicting the sound speed distributions (computed) have been drawn. From these profiles a mean profile considered as a reference profile has been worked out (Fig. 2). The mean sound speed profile shows higher speeds, around 1542.6 m/s at the surface and 1523.6 m/s near the bottom. A minimum sound speed of about 1493.9 m/s occurs around 1750 m depth.

Considering this reference sound speed profile as the base, the range-independent nature of the ocean forward model is solved for preparation of data kernel and predicting travel times (Table 2 (a)).

After completing the above, in order to provide the necessary test data on travel-time perturbations for the inverse model, the winter mean profile has been chosen as the assumed profile to generate possible perturbations in travel times. Numerical experiments have been conducted considering different ocean layers

Table 2(a). Results of computations in noise-free data

No. of rays = 17; No. of layers = 6; No. of factors = 5
 Travel-time data

.0262 .0330-.0552-.1171-.0377-.0377 .0035 .0007 .0330
 .0388 .0190 .0383 .0369 .0381 .0317 .0287 .0262

Data - kernel

.28485E+02 .33904E+02 .29815E+02 .53191E+02 .84437E+02 .72057E+02
 .30233E+02 .55343E+02 .41340E+02 .64383E+02 .10981E+03 .00000E+00
 .29458E+02 .67507E+02 .39682E+02 .60598E+02 .10352E+03 .00000E+00
 .00000E+00 .86665E+02 .49406E+02 .67874E+02 .96650E+02 .00000E+00
 .00000E+00 .00000E+00 .11769E+03 .96955E+02 .85835E+02 .00000E+00
 .00000E+00 .00000E+00 .73707E+02 .13498E+03 .91633E+02 .00000E+00
 .00000E+00 .00000E+00 .00000E+00 .22513E+03 .75040E+02 .00000E+00
 .00000E+00 .00000E+00 .00000E+00 .26601E+03 .34072E+02 .00000E+00
 .00000E+00 .00000E+00 .00000E+00 .30001E+03 .00000E+00 .00000E+00
 .00000E+00 .00000E+00 .00000E+00 .27320E+03 .26888E+02 .00000E+00
 .00000E+00 .00000E+00 .20004E+02 .19358E+03 .86640E+02 .00000E+00
 .00000E+00 .00000E+00 .71623E+02 .13724E+03 .91464E+02 .00000E+00
 .00000E+00 .48621E+02 .58087E+02 .77594E+02 .11628E+03 .00000E+00
 .00000E+00 .84992E+02 .49533E+02 .69466E+02 .96612E+02 .00000E+00
 .28825E+02 .66808E+02 .39553E+02 .61975E+02 .10362E+03 .00000E+00
 .24251E+02 .46156E+02 .33821E+02 .59513E+02 .13730E+03 .00000E+00
 .28151E+02 .33439E+02 .29498E+02 .53364E+02 .83148E+02 .74325E+02

Sum of the diagonal elements of matrix A = .63403510E+06

	E(I)	Closeness ratio
Eigen value No. 1	.490E+06	.77329440E+00
Eigen value No. 2	.113E+06	.95130920E+00
Eigen value No. 3	.148E+05	.97463330E+00
Eigen value No. 4	.102E+05	.99078120E+00
Eigen value No. 5	.463E+04	.99808370E+00

Eigen vectors

-.3764E-01 -.1240E+00 -.1815E+00 -.8832E+00 -.4117E+00 -.2813E-01
 .1240E+00 .3976E+00 .3705E+00 -.4597E+00 .6858E+00 .8720E-01
 -.2362E+00 -.5730E+00 .7311E+00 -.4425E-01 -.1399E-01 -.2814E+00
 .2066E+00 .4329E+00 -.6364E-01 .1579E-01 -.5762E-01 -.8731E+00
 -.1064E+00 .5558E+00 .5113E+00 -.7598E-01 -.5667E+00 .3023E+00

Sum of 5 eigen values = .63282010E+06

Matrix V(trrspose) XV

.1000E+01 -.1288E-06 .9529E-07 -.1969E-07 .3920E-07
 -.1288E-06 .1000E+01 .2235E-06 .3148E-07 .5716E-07
 .9529E-07 .2235E-06 1000E+01 .1966E-07 .2367E-06
 -.1969E-07 .3148E-07 .1966E-07 .1000E+01 .5399E-07
 .3920E-07 .5716E-07 .2367E-06 .5399E-07 1000E+01

Generalised solution

-4.852344E-001; 9.722964E-001 1.1879250;
 -6.755120E-002; -8.519714E-001 5.458165E-001

(4 to 8) to infer the optimum number of layers for reproducing the sound speed profile with utmost accuracy.

32 km range (approx) due to ray bending caused by the refraction at the upper as well as lower boundaries. The extent of the upper and lower limits of the channel correspond to depths of 180 and 3300 m respectively. The duration of ray arrivals spreads over 420 ms. Rays with emergence angles between 5° and 6° arrive early compared to the near-axial ones. Rays with emergence angles exceeding 6° arrive last as obtained from the forward model.

7. RESULTS AND DISCUSSION

As expected, it has been found that the range of variation in the ray loop lengths lies between 50 to 70 km. Ray convergence regions could be seen at every

Table 2(b). Computation in the of noise

No. of rays = 17; No. of layers =4; No. of factors = 4; noise = .0001

Travel-time data

.0262 .0330 -.0552 -.1171 -.0377 -.0377 .0035 .0007 .0330
 .0388 .0190 .0383 .0369 .0381 .0317 .0287 .0262

Sum of the diagonal elements of matrix A + .71317230E06

	E(I)	Closeness ratio
Eigen value No. 1	.693E+06	.97111230E+00
Eigen value No. 2	.113E+06	.98865420E+00
Eigen value No. 3	.148E+05	.99726240E+00
Eigen value No. 3	.148E+05	.10000020E+00

Sum of 4 Eigen values = .71317380E+06

Eigen vectors

-.4337E-01 .7667E+00 -.6398E+00 -.3049E-01
 -.3832E+00 .2976E+00 -.2915E+00 -.8244E+00
 -.5486E-00 .5558E+00 -.6847E+00 -.4682E+00
 .9210E+00 .1208E+00 -.1922E+00 -.3165E+01

Matrix V(trrsspose) XV

.1000E+01 .2995E-07 .6231E-07 .1252E-07
 .2995E-07 .1000E+01 -.4702E-07 -.6559E-08
 .6231E-07 -.4702E-07 .1000E+01 -.1618E-07
 .1252E-07 -.6559E-08 -.1618E-07 .1000E+01

Generalised solution

7.151362E-001; .5748040; -2.0042110 -4.939731E-001

Table 3. Solutions of various modes for six- and four-layer numerical experiments

Tomographic layers (m/s)	Reference assumed		4 modes sound speed (m/s)	Deviation (%)	Through inversion		6 modes sound speed (m/s)	Deviation (%)	Sound speed gradient (s)
	Sound speed (m/s)	Sound speed (m/s)			5 modes sound speed (m/s)	Deviation (%)			
<i>Six-layer numerical experiment</i>									
0- 400	1508.32	1507.84	1507.99	0.009	1507.83	0.001	1507.01	0.055	0.1007
400- 800	1500.75	1501.72	1500.88	0.055	1501.72	0.000	1501.76	0.002	0.0075
800- 1200	1497.55	1498.73	1497.96	0.051	1498.73	0.000	1498.58	0.010	0.0082
1200- 2000	1494.86	1494.77	1494.67	0.066	1494.79	0.001	1494.76	0.001	0.0020
2000- 3000	1503.35	1502.50	1503.35	0.056	1502.49	0.001	1502.66	0.010	-0.0122
3000- 4000	1523.60	1523.04	1522.59	0.029	1523.05	0.001	1523.26	0.014	-0.0167
<i>Four-layer numerical experiment</i>									
0- 400	1508.32	1507.84	1508.40	0.037	1507.75	0.005	1509.03	0.078	0.1010
400- 1750	1497.70	1498.14	1498.00	0.009	1499.10	0.064	1499.27	0.075	0.0620
1750- 3000	1500.46	1500.50	1500.07	0.028	1498.72	0.118	1498.45	0.136	0.0100
3000- 4000	1523.60	1523.60	1522.62	0.064	1523.54	0.003	1523.10	0.032	0.0170

The ray travel-time deviations between the reference and perturbed cases show variations between 0.7 ms and 117 ms (Table 2 (a)). The positive perturbations in sound speed gives rise to negative perturbations in travel time and vice versa. The ray path lengths (km) covered by 17 eigen rays in each of the six tomographic layers (Table 2 (a)) indicate diverse sampling by the eigen rays in each of the layers. The upper 180 m of the water column has not been sampled due to depth limited nature of the sound speed profile. Realising that only six layers are chosen and more number (17) of rays prevail, the system of equations in Eqn (11) becomes over-determined. A solution for this can be obtained by treating the data over the entire water column in a way similar to that of a solution under least square sense.

Using the data kernel, singular value decomposition has been performed, and the generalised inverse operator computed. Travel-time perturbations are used by the generalised inverse operator to obtain the inverse solution (Table 2).

The generalised inverse solutions for a typical, pre-set number of layers, viz. for 6-and 4-layer models have been worked out considering different energetic modes (4 to .6). The deviations between the reconstructed and the perturbed/assumed profiles are obtained (Table 3). From this, it can be noticed that for the case of six-layer numerical experiment, by considering five energetic modes, the reconstructed profile of sound speed is well in agreement with that of the assumed profile.

The closeness ratio (ratio between the sum of the factor model and sum of the data matrix/data kernel, presented in Table 4) indicated that the first five modes

Table 4. Eigen values and corresponding closeness ratio for six- and four-layer mode

Six-layer model		Four-layer model	
Eigen value	Closeness ratio		Closeness ratio
0.490×10^6	77.32	0.693×10^6	97.11
0.113×10^6	17.81	0.125×10^5	1.75
0.148×10^5	2.33	0.614×10^4	0.86
0.102×10^5	1.51	0.195×10^4	0.28
0.463×10^4	0.73		
0.121×10^4	0.20		100.00
	100.00		

(arranged in descending order) gave rise to 99.8 per cent information. This enabled reproduction of the original profile. By considering six modes, a small eigen value term which is present in the denominator of the Eqn (18) has amplified the noise instead of increasing the accuracy of the solution.

This is due to the fact that the eigen values are arranged in descending order and as the singular values decrease in size (l^2), the structure of the corresponding eigen vectors (columns of U and V) becomes more complex and wavelike in nature. The eigen vectors corresponding to the largest eigen value indicate that the large scale features can best be determined. As the

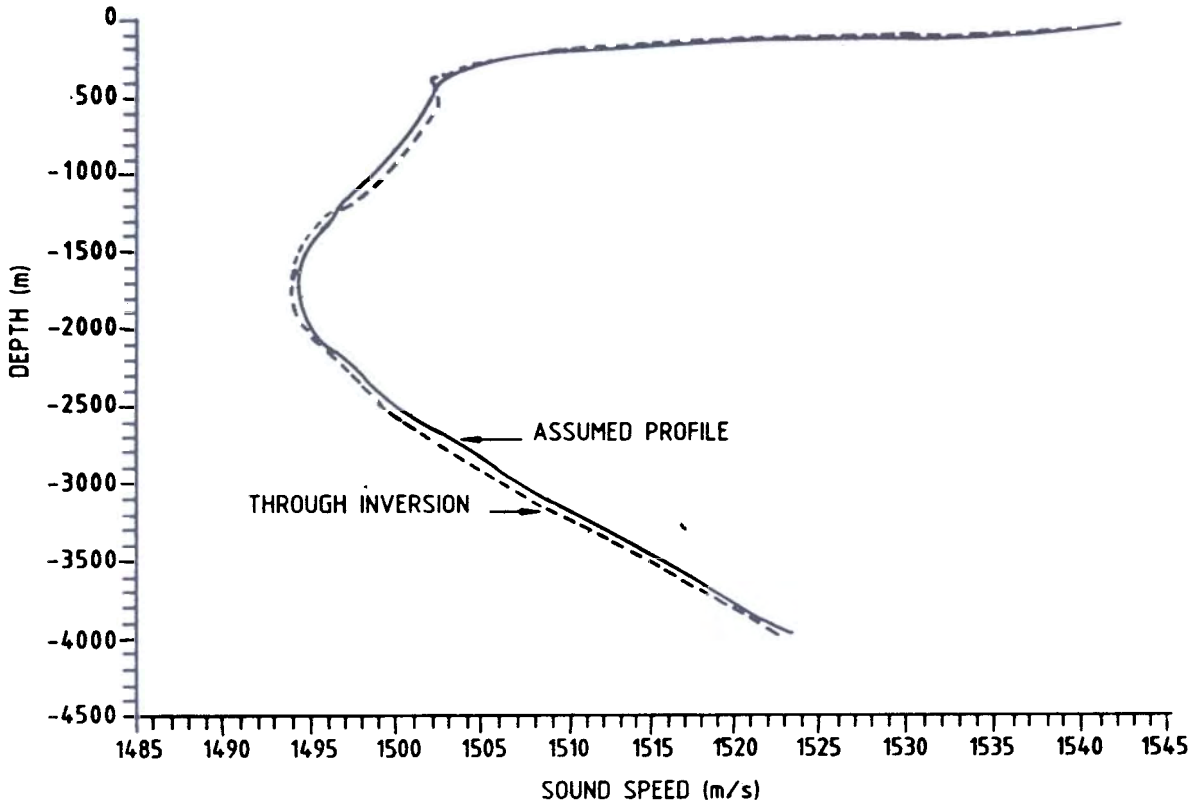


Figure 5. Assumed and reconstructed sound speed profiles for a six-layer model.

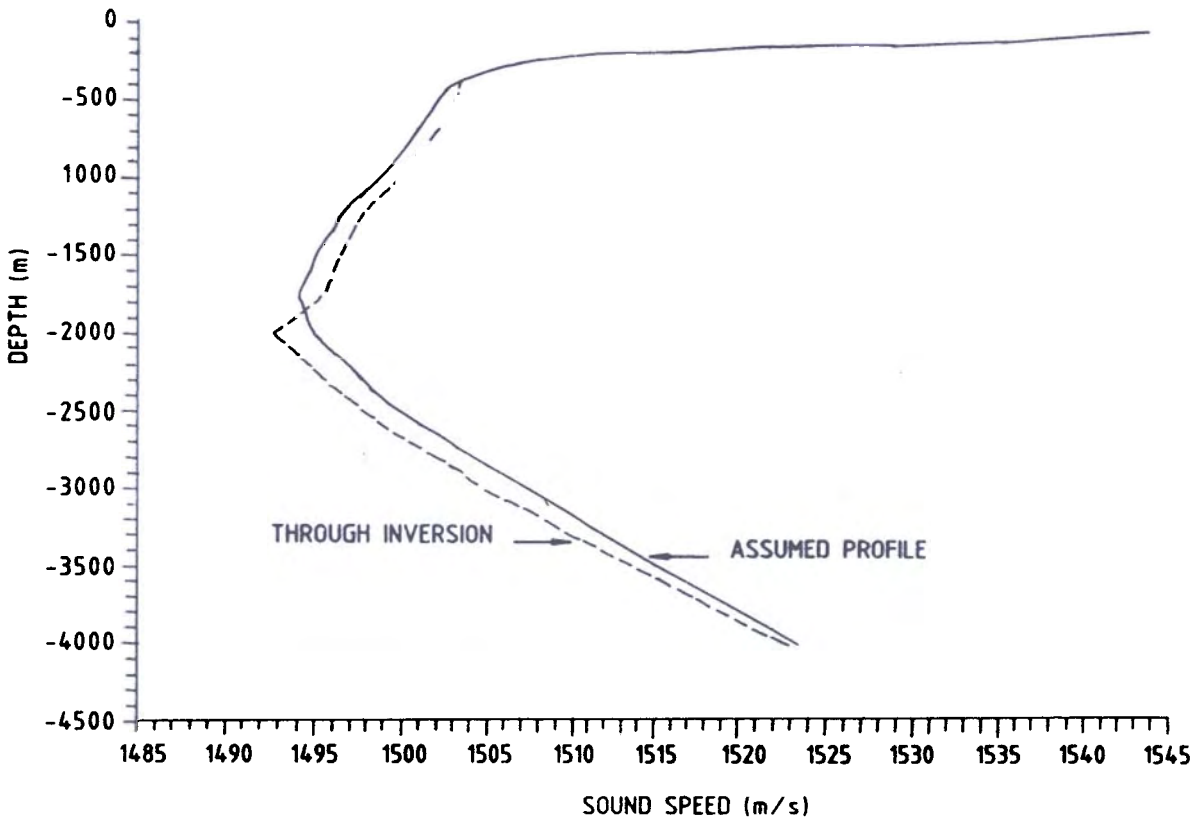


Figure 6. Assumed and reconstructed sound speed profiles for a four-layer model.

eigen vectors corresponding to smaller and smaller eigen vectors are incorporated, smaller scale features surface in the inverse estimates. These features cannot be determined like the large scale features due to the inverse of the l^2 of Γ .

The assumed initial profile and the reconstructed one with five modes for the six-layer numerical experiment have been shown in Fig. 5. The two profiles are close to each other. Similar exercise carried out for a four-layer model with two modes (Fig. 6) showed more departures indicating the usefulness of the six-layer model over the four-layer one.

The effect of noise arising from the horizontal movements of the moorings, on which the sensors are suspended, when expressed in terms of travel-time differences/perturbations resulted in negligible per cent change in the reconstructed sound speed profile. For example, a travel-time difference of 0.0001 s (Table 2 (b)) in the form of noise yielded a change of 0.1 per cent of the sound speed as seen from the corresponding values in the respective layers (Table 3) for a four-layer case.

ACKNOWLEDGEMENTS

The authors are thankful to the Director, NIO, for his keen interest in this study. This study forms a part of the grant-in-aid project by the Department of Ocean Development, Govt of India, New Delhi.

REFERENCES

1. Munk, W.H. & Wunsch, C. Ocean acoustic tomography: a scheme for large scale monitoring. *Deep Sea Res.*, 1979, **26(A)**, 123-61.
2. Menke, W. Geophysical data analysis: discrete inverse theory. Academic Press, New York, 1984. p. 260.
3. Officer, C.B. Introduction to the theory of sound transmission. McGraw-Hill, New York, 1958. p. 284.
4. Carnhan, B.; Luther, H.A. & Wilkes, J.O. Applied numerical methods. John Wiley, New York, 1969. p. 604.
5. Backus, G.E. & Gilbert, J.E. Numerical application of a formalization for geophysical problem. *Geophys. J.*, 1967, **13**, 247-76.
6. Wiggins, R.A. The general linear inverse problem: implication of surface waves and free oscillations for earth structure. *Rev. Geophys. and Space Phys.*, 1972, **10**, 251-85.
7. Parker, R.L. Understanding inverse theory. *Ann. Rev. Earth and Planet. Sci.*, 1977, **5**, 35-64.
8. Wunsch, C. The Atlantic general circulation west of 50° W determined by inverse methods. *Rev. Geophys. and Space Phys.*, 1978, **16**, 583-620.
9. Roemmich, D. Circulation of the Caribbean Sea: a well resolved inverse problem. *J. Geophys. Res.*, 1981, **86**, Bi (C9), 7993-8005.
10. Fu, Lee-Lueng. The general circulation and meridional heat transport of the subtropical south Atlantic determined by inverse methods. *L. Phys. Oceanogr.*, 1981, **11(9)**, 1171-93.
11. Cornuelle, B. Inverse methods and results from the 1981 ocean acoustic tomography experiment. Massachusetts Institute of Technology/Woods Hole Oceanographic Institution, 1983. Ph.D Thesis, 359 p.
12. Cornuelle, B.; Wunsch, C.; Behringer, D.; Birdsall, T.; Brown, M.; Heinmiller, R.; Knox, R.; Metzger, K.; Munk, W.; Spiesberger, J.; Spindel, R.; Webb, D. & Worcester, P. Tomographic maps of the ocean mesoscale: pure acoustics. *J. Phys. Oceanogr.*, 1985, **15**, 133-52.
13. Lanczos, C. Linear differential operators. Van Nostrand, Princeton, 1961. p. 564.
14. Jackson, D.D. Interpretation of inaccurate, insufficient and inconsistent data. *Geophys. J. Soc.*, 1972, **28**, 97-109.
15. Wiggins, R.A.; Lerner, K.L. & Wisecup, R.D. Residual static analysis as a general linear inverse problem. *Geophys. J.*, 1976, **41**, 922-38.

16. Wunsch, C. Tracer inverse problems. *In* Oceanic circulation models: combining data and dynamics, edited by D.L.T. Anderson & J. Willebrand. Kluwer Academic Publishers, Hingham, 1989. pp. 1-77.
17. Tarantola, A. Inverse problem theory: methods for data fitting and model parameter estimation. Elsevier, Amsterdam, 1987. p. 613.
18. Ramana Murthy, T.V.; Veerayya, M. & Murthy, C.S. Sediment-size distributions of the beach and nearshore environs along the central west coast of India: an analysis using EOF. *J. Geophys. Res.*, 1986, **91**(C7), 8523-36.
19. Ralston, A. (Ed). Mathematical methods for digital computers, John Wiley, New York, 1966. p. 293.
20. Chen, C.T. & Millero, F.J. Speed of sound in sea water at high pressure. *J. Acoust. Soc. Am.*, 1977, **62**(5), 1129-35.